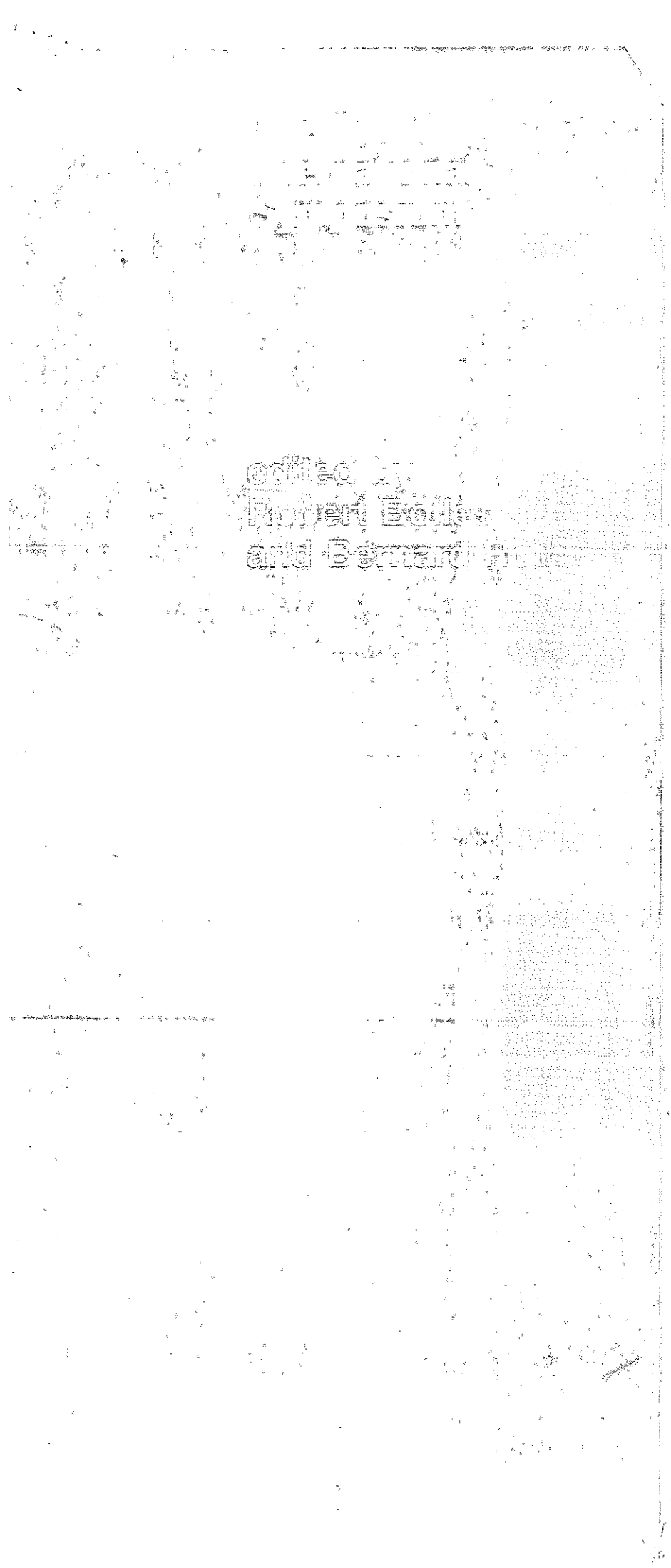

Robotics Research:
The Fourth International Symposium
edited by Robert Bolles and Bernard Roth

The Fourth International Symposium on Robotics Research was held in the summer of 1987 in Santa Cruz, California. This book collects 52 contributions by prominent researchers from Japan, Europe, and the United States. The topics covered include kinematics and dynamics, mobile robots, design and mechanisms, and perception.

Selected contents: ROBOTWORLD: A Multiple Robot Vision Guided Assembly System (Scheinman). Investigating Fast, Intelligent Systems with a Ping-Pong Playing Robot (Andersson). Behavior Based Design of Robot Effectors (Jacobsen, et al.). Intrinsic Tactile Sensing for Artificial Hands (Bicchi, Dario). Whole Arm Manipulation (Salisbury). Grasping as a Contact Sport (Cutkosky, et al.). MEISTER: A Model Enhanced Intelligent and Skillful Teleoperational Robot System (Sato and Hirai). Optical Range Finding Methods for Robotics (Idesawa). 4D-Dynamic Scene Analysis with Integral Spatio-Temporal Models (Dickmanns).

Model-Based Object Motion Tracking (Mundy, Thompson). Sensor-Based Manipulation Planning as a Game with Nature (Taylor, Mason, Goldbert). Issues in the Design of Off-Line Programming Systems (Craig). HANDEY: A Task-Level Robot System (Lozano-Perez, et al.). Design and Sensor-Based Robotic Assembly in the "Design to Product" Project (Fehrenbach, Smithers). Collision Detection among Moving Objects in Simulation (Kawabe, Okano, Shimada). An Automated Guided Vehicle with Map Building and Path Finding Capabilities (Jarvis, Byrne).

Robert Bolles is a Staff Scientist at SRI International. Bernard Roth is Professor of Mechanical Engineering at Stanford University. *Robotics Research: The Fourth International Symposium* is included in the Artificial Intelligence Series edited by Patrick Winston and Michael Brady.

Robotics Research

The Fourth International Symposium

edited by

Robert C. Bolles

and

Bernard Roth

The MIT Press
Cambridge, Massachusetts
London, England

INTRINSIC TACTILE SENSING FOR ARTIFICIAL HANDS

A. Bicchi[0^] and P. Dario[0]

[0] Centro "E. Piaggio", Faculty of Engineering, University of Pisa, Italy
[^] Dipartimento di Ingegneria delle Costruzioni, University of Bologna, Italy

In this paper "intrinsic" tactile sensing, i.e. contact sensing based on pure force and torque measurements and geometric calculations, is discussed with reference to the design of sensorized fingertips for artificial hands. Pros and cons of the intrinsic approach are examined, as opposed to "extrinsic" tactile sensing systems, usually consisting of sensitive arrays distributed over the sensor surface. While either sensing method could prove best for specific applications, the integration of the two for a general-purpose artificial fingertip sensor is recommendable. Some general considerations are made about the design of intrinsic tactile sensing systems, and the derived guidelines used for the development of an intrinsic sensor conceived to be a part of a multifunctional sensorized finger. A description of this sensor is provided in the paper along with the experimental evaluation of its performances.

INTRODUCTION

Dexterous manipulation and haptic perception are the fundamental aims of the evolution of present robotic end effectors toward a future artificial hand system, even if the development of end effectors intended for carrying out those two functions has proceeded thus far along almost distinct pathways |Dario 1987|.

The design of an artificial hand system requires substantial progresses in three main areas: actuators for hand motion, sensors of the actual state of the hand-environment system, and AI techniques for managing the perceptual and decisional processes, involved in manipulatory tasks.

In the sensing domain, we can distinguish between proprioceptive sensing (i.e. getting information on the hand itself, such as joint angles or torques) and exteroceptive sensing, which is related to the interactions between the hand and its environment. In the hand (both human and robotic), exteroceptive sensing is essentially distributed force sensing, although other sensing capabilities (such as proximity, temperature, chemical, etc.) could be also implemented.

In this paper we discuss some different aspects of tactile sensing for artificial hands and pursue solutions to the dual requirements of controlling robotic manipulation and perception.

So far, artificial tactile sensing has been investigated mostly through an "extrinsic" approach (i.e. by means of pressure sensing arrays distributed over the sensor surface). Harmon |1982| showed as most research efforts have been directed to replicate the sensory properties of the human skin, by spreading sensing sites over the hand surfaces where contacts with the environment are expected to occur ("active surfaces").

On the other hand, "intrinsic" tactile sensing is contact sensing based on pure force and torque measurements and geometric calculations, as proposed first by J.K. Salisbury |1984|. The tactile system developed by Salisbury had no distributed sensing capabilities in the active surface, but rather a force sensing device remote from the contact, and the software means necessary to infer the desired tactile information from force data.

A summary of the possible advantages and drawbacks of tactile sensors of the two classes is proposed in Table 1.

TYPE FEATURES	EXTRINSIC	INTRINSIC
SPATIAL RESOLUTION	INHERENTLY FINITE	THEORETICALLY INFINITE
BANDWIDTH	LIMITED	HIGH
CONTACT FORCE MEASUREMENT	GENERALLY INACCURATE	FAST,LINEAR, NONHYSTERETIC
FRICTIONAL EFFECTS	AT PRESENT, NOT SENSED	MEASURED
SLIPPAGE DETECTION	NONE	POSSIBLE
SENSOR SURFACE SHAPE	FREE	ONLY SIMPLE SHAPES
SENSOR COVER COMPLIANCE	ALLOWED	IT PRODUCES ERRORS
PARATACTILE SENSITIVITY	POSSIBLE	IMPOSSIBLE
ENCUMBRANCE	MANY WIRES	RATHER BULKY, FEW WIRES

TABLE 1

An intrinsic tactile sensor (ITS) is very useful for manipulation control, because it is able to monitor the resultant of contact forces in real time. For this reason, an ITS is suitable for such tasks as object contouring, assembly operations, etc.

ITS handles very well also frictional forces, whose effects it can distinguish and measure. Based on this information, if a proper model of friction between the sensor's active surface and the body is available, an "a priori" strategy can be selected to prevent slippage.

If the contact can be hypothesized as punctual, i.e. if the contacting surfaces are rigid enough and have different spatial curvatures, and if the contact takes place in no more than one point at a time, the ITS can resolve with high (theoretically infinite) spatial resolution the contact point.

Conversely, an extrinsic tactile sensor (ETS) has inherently finite spatial resolution and it is not able, in general, to sense frictional forces, by which it is often even deceived.

An advantage of ETSs is that they are capable of managing contacts, over large areas, which are likely to occur if a very compliant fingertip cover is used to enhance grasp stability. Furthermore, an ETS permits the extraction of "tactile images", which are very useful in order to recognize local features of objects.

A few ETS also incorporate sensing elements capable of detecting some very useful "paratactile" characteristics, such as the thermal properties of the object being touched |Dario et al. 1984||Siegel 1986|.

In this paper some general issues related to the design of an ITS are discussed, and the fabrication and testing of a prototype of such sensor are described some preliminary work aimed at integrating this ITS sensor with the ETSs being developed in our laboratory is also outlined.

GENERAL CONSIDERATIONS ON "INTRINSIC" TACTILE SENSING

Basically, an ITS system consists of three elements: a force sensor, an active surface, and an electronic computing unit.

A force sensor is a device which measures, in a particular coordinate frame, the six components of the generalized (force and torque) force vector which is exerted through the sensor itself. Similar devices have been already studied and applied in robotics, mostly as sensorized pedestals or wrists |Bejczy 1983|.

The active surface of a sensor is the set of points where the contacts with the environment are expected to occur. In an ITS, the active surface is integral with the force sensor, to which the mechanical effects of the contact forces are transmitted.

An accurate geometrical description of the active surface in the force sensor coordinate frame is mandatory.

Although there are infinite load configurations statically equivalent to a given generalized resultant force vector, there is only one such pure force (no torque).

With reference to Figure 1, let F_1-F_6 be the resultant force components which are sensed by the force sensor along its coordinate frame axes X_1,X_2,X_3.

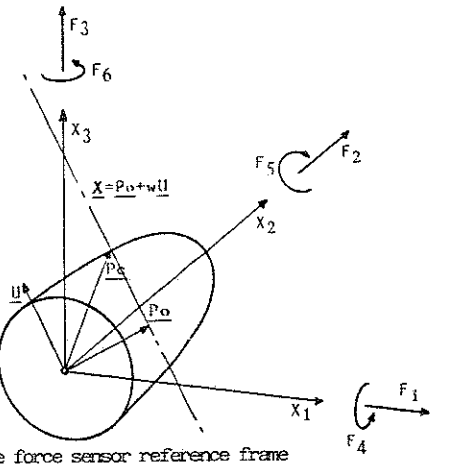

FIG.1. The force sensor reference frame

If a pure force load is assumed (i.e., if punctual contacts transmitting no local torques are hypothesized), then such force must lay on the line |Salisbury 1984|:

$$\underline{X} = \underline{Po} + w\,\underline{U} \qquad 1)$$

where:

$$\underline{Po} = \left(\frac{F_2F_6 - F_3F_5}{|\underline{F}|^2} \; ; \; \frac{F_3F_4 - F_1F_6}{|\underline{F}|^2} \; ; \; \frac{F_1F_5 - F_2F_4}{|\underline{F}|^2} \right)$$

$$\underline{U} = \frac{1}{|\underline{F}|}\,(F_1;F_2;F_3)$$

$$|\underline{F}|^2 = (F_1^2+F_2^2+F_3^2)$$

Intersecting this line with the active surface $f(X_1,X_2,X_3)=0$, so as to obtain the value of w corresponding to the contact point, is the task of the computing unit of an ITS system.

In the particular case of a spherical active surface, having its center in the origin of the force sensor coordinate frame, and radius R, the expression for w is:

$$w = \pm \left(R^2 - \frac{(F_2F_6-F_3F_5)^2-(F_3F_4-F_1F_6)^2-(F_1F_5-F_2F_4)^2}{|\underline{F}|^4} \right)^{\frac{1}{2}} \qquad 2)$$

and the contact point $\underline{Pc} = (X_1,X_2,X_3)$ can be calculated from (1). The sign ambiguity in (2) is easily solved, if only compressive forces are assumed on the active surface.

It is apparent that the spatial resolution of an ITS is only theoretically infinite, even in the point-contact hypothesis. In fact, the ultimate resolution is limited by the errors with which the above expressions are calculated. Assuming that the errors made in the determination of the geometric constants of the active surface are small with respect to the inaccuracies in force measurement, the criteria for the error propagation in algebraic calculations give the following upper limit for the error:

$$\frac{|d\underline{F}|}{|\underline{F}|} \leq 2 \max \frac{|dFi|}{|Fi|} \; ; \; i=1,3 \; = 2\,Ef \qquad 3)$$

$$|dX_1| \leq \frac{2}{|\underline{F}|^2}\,Ef\;2(|F_2F_6|+|F_3F_5|) + K\,|F_1| \qquad 4)$$

$$|dX_2| \leq \frac{2}{|\underline{F}|^2}\,Ef\;2(|F_3F_4|+|F_1F_6|) + K\,|F_2| \qquad 5)$$

$$|dX_3| \leq \frac{2}{|\underline{F}|^2} \; Ef \; 2(|F_1F_5|+|F_2F_4|) + K\,|F_3| \qquad 6)$$

where:
"|Q|" is the absolute value of the scalar quantity "Q"
"dQ" indicates the absolute error on the quantity "Q";

$Ef = \max \frac{|dFi|}{|Fi|}$; i=1,6 is the maximum relative error made by the sensor in the measurement of $F_1 - F_6$;

$$K = \frac{|\underline{F}|^2 R^2 + 2\,(|F_2F_6|+|F_3F_5|)^2 + (|F_3F_4|+|F_1F_6|)^2 + (|F_1F_5|+|F_2F_4|)^2}{w\,|\underline{F}|}$$

It should be pointed out that the foregoing expressions have been actually evaluated neglecting the errors due to the use of finite precision computing units.

The application of (3)-(6) to the cases of contact with and without friction will help in understanding the entity of such errors:

Case a): Contact without friction ($F_4=F_5=F_6=0$);

$$|dXi| \leq 2\,R\,\frac{|Fi|}{|\underline{F}|}\,Ef\,, \quad i=1,3 \qquad 7)$$

The maximum error in the localization of the contact point is:

$$|d\underline{P}| \leq (dX_1^2+dX_2^2+dX_3^2)^{\frac{1}{2}} \doteq 2\,R\,Ef \qquad 8)$$

For example, with R=10 mm, Ef = 1%, the accuracy is 0.2 mm; the maximum angular error in the determination of the contact force vector ($|d\underline{P}|/R$) is 1 degree.

Case b): Contact with friction.
Let, for example, $F_1=Fo\cos(q)$, $F_2=Fo\,sen(q)$, $F_3=F_4=F_5=0$, $F_6=R\,Fo\,sen(q)$, where "tang(q)" is the Coulomb friction coefficient. Then:

$$|d\underline{P}| \leq 2\,R\,Ef\,f(q) \quad \text{where} \quad \begin{array}{l} f(q)= 1.08 \text{ for } tang(q)=0.1 \\ f(q)= 1.62 \text{ for } tang(q)=0.3 \\ f(q)= 2.30 \text{ for } tang(q)=0.5 \end{array} \qquad 9)$$

It appears from these expressions that the precision of an ITS is essentially related to the accuracy of the force sensor (1/Ef). Owing to this fact and to the problems associated with the miniaturization of the sensing device, the development of an ITS system requires extreme attention to the design of the force sensor.

FORCE SENSORS FOR "INTRINSIC" TACTILE SENSING

A force sensor consists of a mechanical structure fixed to a rigid frame at one end, while an external force system is applied to the other end. When the classical linear elasticity hypotheses hold, it is possible to deduce the state of stress, and ultimately the load originating it, from strain measurements.

The state of strain in a point of a mechanical structure is described by 6 components of the strain tensor; in general they are correlated to the stress tensor through relations accounting also for the effects of temperature. However, most available strain transducers measure only one component of the strain tensor along some peculiar direction; moreover, the temperature effects on strain are most often kept under control by means of "dummy" transducers, or even inherently compensated for. Thus, the electrical output Vi of the i-th strain transducer can be written:

$$Vi = Gi\sum_{j=1}^{6} Aij\,Fj = \sum_{j=1}^{6}\left[Gi\;Aij\;|Fj,n|\right]\left[\frac{Fj}{|Fj,n|}\right] = \sum_{j=1}^{6} Cij\,Pj \qquad 10)$$

where Gi is the transducer conversion factor and Aij depend on the geometry and elastic properties of the sensor structure. In order to normalize these equations, in (10) are introduced the "nominal values" Fj,n of the components F_1-F_6, i.e. the maximum values that those quantities are supposed to attain during the task operations |Von Brussel et al. 1985|.

If several such transducers are placed in the mechanical structure of the force sensor, we obtain a linear algebraic system, expressed in matrix notation as:

$$\underline{V} = C\,\underline{P} \qquad 11)$$

Some methods of linear algebra can be applied to this system in order to study the optimal configurations of a force sensor. In general, at least 6 strain transducers are needed to solve Eq.(13) for the six components of $\underline{P}$, provided that those transducers are placed so that the rows of the C matrix are linearly independent. We say that a force sensor using just 6 transducers has a "minimal" configuration, as opposed to "extended" configurations using more transducers.

The attention of the investigators who dealt with the development of force sensing devices has been focused thus far mostly on "extended" configurations |Bejczy 1983| |Von Brussel et al. 1985| |Brock and Chiu 1985| |Hirzinger 1987|. The requirements in terms of simplicity, low cost and small number of wires, for a force sensor to be incorporated in a robot end effector suggest, instead, to investigate "minimal" force sensor configurations.

According to (13), we might place arbitrarily 6 strain transducers on whatever mechanical structure to build a force sensor (excluding the unlikely case in which the associated matrix "C" is singular). The Cij components of the matrix C may be calculated by means of the elasticity theory relations in any but the simplest cases. However, it is possible to evaluate those components with an accurate calibration of the sensor, consisting in the application of well known loads and in the measurement of the responses of each basic transducer to each component of $\underline{P}$.

Once the matrix C associated with the sensor is known, an algorithm can be written to solve for $\underline{P}$ any $\underline{V}$ measurement: Gaussian elimination is generally the preferable method |Wilkinson 1965|.

Any configuration of 6 basic transducers will be then equally suitable for a force sensor? The answer is no, of course. Optimization criteria for the disposition of the 6 basic transducers are provided by the analysis of the force sensor accuracy. Both $\underline{V}$ and C are not known with absolute precision. Measuring transducer signals generally implies electrical noise and analog-to-digital conversion inaccuracies: a relative error is defined as the ratio of the norm of the error vector $d\underline{V}$ to the norm of the measurements vector $\underline{V}$:

$\|d\underline{V}\|/\|\underline{V}\|$ (the Euclidean norm, indifferent to reference changes, is the preferable choice in this case). Also the calibration operations, notwithstanding the care one can pay, introduce some errors in estimated Cij. A relative error on C is defined as $\|dC\|/\|C\|$, where the definition of spectral norm is assumed. From the theory of linear systems solution [Wilkinson 1965], we observe that these errors "propagate" through the algorithms to the solution $\underline{P}$, being amplified by the "condition number" Nc of the C matrix:

$$\frac{\|d\underline{P}\|}{\|\underline{P}\|} \leq \left(\frac{\|d\underline{V}\|}{\|\underline{V}\|} + \frac{\|dC\|}{\|C\|} \right) \frac{Nc}{1 - Nc\,\|dC\|/\|C\|} \qquad 14)$$

where: $Nc = \|C\|\,\|C^{-1}\|$

The condition number of a matrix is always greater than, or equal to, 1; the latter case occurs only when the matrix has orthogonal columns. A well conditioned sensor, having small Nc, will not magnify the errors intrinsic to its fabrication. It should be noted that, while decreasing $\|d\underline{V}\|/\|\underline{V}\|$ and $\|dC\|/\|C\|$ is a matter of instrumentation quality (thus, ultimately, of mere cost), Nc depends only on the quality of the sensor design. Small Nc guarantee also other good qualities to the sensor, such as uniform accuracy over the whole allowed range of contact points and contact force intensities. Hence, the number 1/Nc can be assumed as a figure of merit for different configurations of basic transducers in a force sensor.

It should be noted that increasing the basic sensitivity of transducers to strain by a constant factor (for instance, by using solid state, instead of foil, strain gauges) would not affect sensor accuracy (as Nc remains unchanged), but only the measurement range, allowing smaller forces to be sensed.

Unfortunately, the condition number of a matrix is, in general, a very involved function of matrix entries. Thus, the optimization of the sensor design is not achievable in close form. Only in particular cases we get some intelligible hints; for instance, if Cis diagonal:

$$Nc(C) = \|C\|\,\|C^{-1}\| = \frac{\max(Cii,\ i=1,6)}{\min(Cii,\ i=1,6)} \qquad 15)$$

Given a minimum Cii (the sensitivity to the force vector component Pi), there is no advantage in having better sensitivities to other components, as this would make accuracy even worse. The equalization of sensitivities is then strongly recommendable, confirming the intuitive guess.

Even in the general case, however, a numerical evaluation of Nc for a certain number of configurations varying about a reference design can help in understanding the roles played by some design parameters. An example of the application of this approach is given in the next paragraph.

DESIGN OF AN ITS FOR ARTIFICIAL FINGERTIPS.

The concept of a fingertip ITS has been recently implemented by Brock and Chiu (1985), who designed a sensor incorporating 16 very sensitive (but costly and fragile) semiconductor strain gauges.

As anticipated in the introduction, our goal in studying IT sensing was the design and realization of a precise, reliable, cost effective device to be integrated in a thoroughly sensorized, real size fingertip for artificial hands. We tried to fulfill the specifications for this application (miniaturization, robustness, low number of connecting cables, in addition to precision and time response) emphasizing sensor simplicity.

We elected to employ strain gauges as "basic" strain transducers in our prototype sensor, since this technique has proved reliable, accurate and economical in innumerable applications. A thin walled cylindrical cantilever beam was chosen as the mechanical structure of the force sensor. The sensor structure is depicted in Figure 2, along with the associated coordinate frame X_1, X_2, X_3.

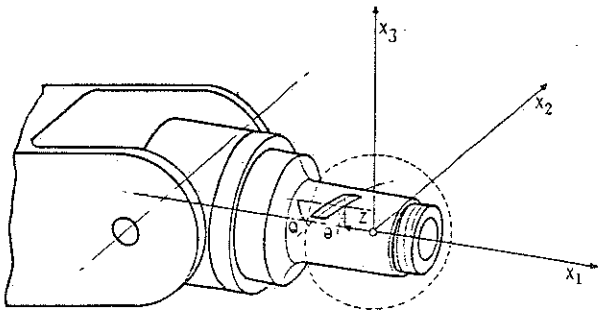

FIG. 2. The mechanical structure of the force sensor. The dashed line sketches the active surface.

In order to realize a "minimal" force sensor, six gages are to be bonded to the beam surface: their position will be uniquely determined by the cylindrical coordinates Z, θ of the strain gauge center, and by the angle Q the gage axis forms with the X axis.

By measuring the unbalancement of a Wheatstone bridge having the i-th gauge as a leg, a signal Vi given by (12) will be obtained:

$$Vi = \sum_{j=1}^{6} Cij\ Pj = G \sum_{j=1}^{6} Aij\ |Fj,n|\ \frac{Fj}{|Fj,n|} \qquad 12')$$

where G is a constant depending upon the gage factor, the excitation voltage and the bridge amplifier gain (which can be reasonably assumed the same for each gage).

Assuming the hypotheses currently adopted in the theory of elasticity in order to describe the strains in a cylindric cantilever beam loaded with normal and shear forces, and with torsional and bending torques, the i-th row of the C matrix can be written as:

$$\begin{aligned}
Ci1 &= G\,|F_1,n|\ \left[\cos^2(Qi) - \mu \sin^2(Qi)\right] Wn \\
Ci2 &= G\,|F_2,n|\ \left\{Zi\ \left[\cos^2(Qi) - \mu \sin^2(Qi)\right] \cos(\theta i)\ Wf + \right. \\
&\quad \left. + \sin(2\,Qi)\ \sin(\theta i)\ Ws \right\} \\
Ci3 &= G\,|F_3,n|\ \left\{Zi\ \left[\cos^2(Qi) - \mu \sin^2(Qi)\right] \sin(\theta i)\ Wf + \right. \\
&\quad \left. + \sin(2\,Qi)\ \cos(\theta i)\ Ws \right\} \\
Ci4 &= G\,|F_4,n|\ \sin(2\,Qi)\ Wt \\
Ci5 &= G\,|F_5,n|\ \left[\cos^2(Qi) - \mu \sin^2(Qi)\right] \cos(\theta i)\ Wf \\
Ci6 &= G\,|F_6,n|\ \left[\cos^2(Qi) - \mu \sin^2(Qi)\right] \sin(\theta i)\ Wf
\end{aligned} \qquad 16)$$

where "μ" is the Poisson coefficient of the beam material, and Wn, Wf, Ws, Wt are constants depending on the elastic properties of the material and on the geometry of the beam section:

$$Wn = \frac{1}{2\,E\,\pi\,R\,s}\ ;\ Wf = 2\,Wn/R;$$
$$Ws = 2\,(1+\mu)\,Wn\ ;\ Wt = (1+u)\,Wn/R \qquad 17)$$

where E is the material Young's modulus, R is the cylinder radius and s the cylinder wall thickness.

The condition number associated with this sensor is a complicated function of the nineteen parameters at designer's disposal (Qi,θi,Zi (i=1,6) and R). This function is by far too complex to be minimized symbolically, although this procedure would have led to the absolute "optimal" sensor in this class.

Thus, we followed a semiheuristic procedure: a basic configuration was chosen "intuitively", and only three parameters Q, d and R, described in Figure 3, were left for optimization.

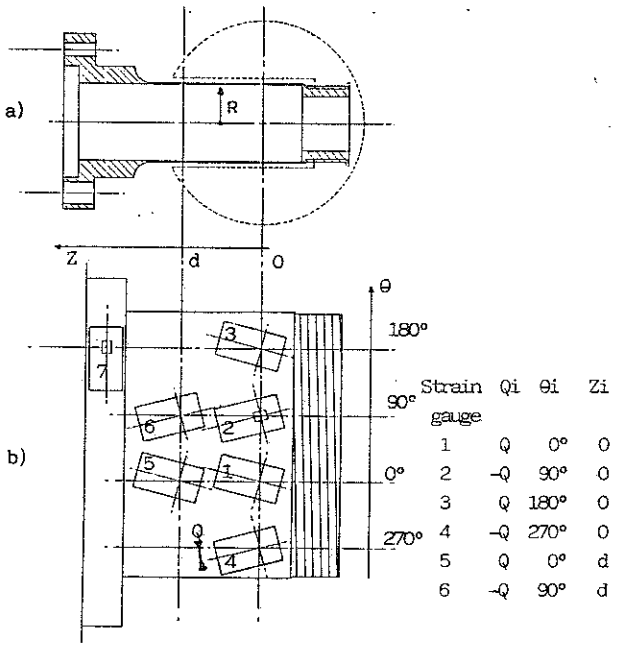

FIG. 3 Cross section a) and plane development b) of the force sensor

Substituting these values in (14), we obtain the C matrix for our sensor:

$$C = \begin{bmatrix} C_1 & 0 & C_3 & -C_4 & 0 & C_6 \\ C_1 & -C_2 & 0 & C_4 & C_5 & 0 \\ C_1 & 0 & -C_3 & -C_4 & 0 & -C_6 \\ C_1 & C_2 & 0 & C_4 & -C_5 & 0 \\ C_1 & C_7 & C_3 & -C_4 & 0 & C_6 \\ C_1 & -C_2 & -C_8 & C_4 & C_5 & 0 \end{bmatrix} \qquad 18)$$

where:

$$C_1 = G\,|F_1,n|\,[\cos^2(Q)-\mu\sin^2(Q)]\,Wn$$
$$C_2 = G\,|F_2,n|\,\sin(2\,Q)\,Ws$$
$$C_3 = G\,|F_3,n|\,\sin(2\,Q)\,Ws$$
$$C_4 = G\,|F_4,n|\,\sin(2\,Q)\,Wt$$
$$C_5 = G\,|F_5,n|\,[\cos^2(Q)-\mu\sin^2(Q)]\,Wf$$
$$C_6 = G\,|F_6,n|\,[\cos^2(Q)-\mu\sin^2(Q)]\,Wf$$
$$C_7 = G\,|F_2,n|\,[\cos^2(Q)-\mu\sin^2(Q)]\,Wf\,d$$
$$C_8 = G\,|F_3,n|\,[\cos^2(Q)-\mu\sin^2(Q)]\,Wf\,d$$

Moving through the space of the parameters Q, d and R, the figure of merit Nc(C) varies unpredictably. However, Nc (C) is likely to have several local minima, while it certainly tends to infinite as C approaches singularities. Notwithstanding that ideal configurations (Nc=1) might well not exist, placing Nc(C) in one of the lowest "hollows" of its locus can be assumed as a design target.

A computer program which, given a set of initial parameters, moves in the parameter space and "tumbles down" into the hollows it encounters, has been purposely written. The flow chart of this optimization program is sketched in Figure 4.

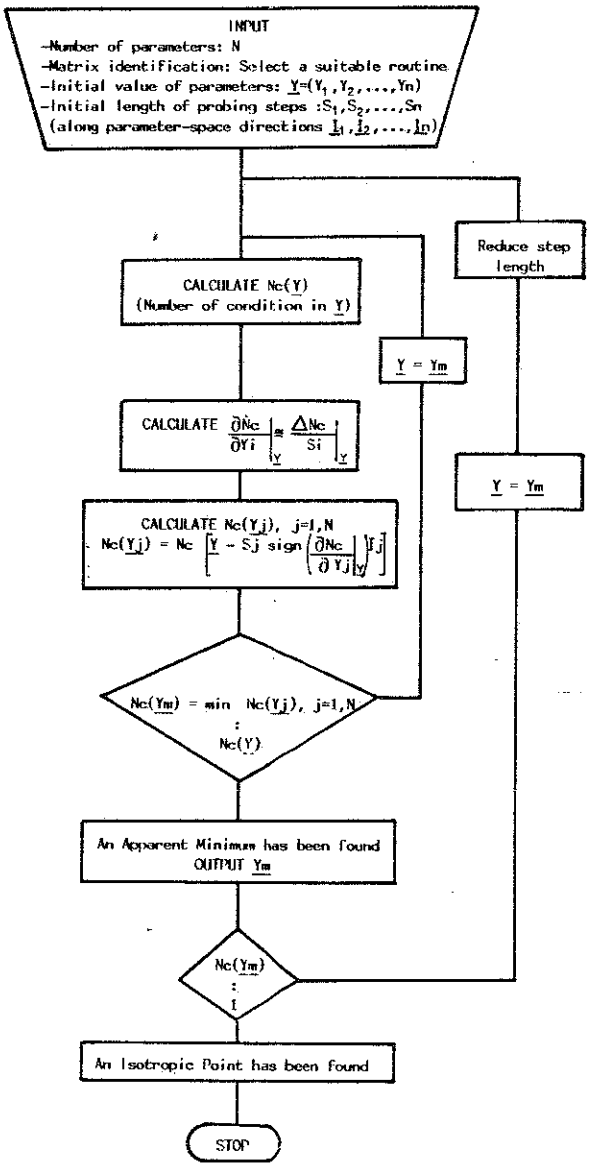

FIG. 4. A simplified flow-chart of the design optimization program

The program, suitable for general matrices with any number of parameters, adapts automatically the probing step length, and it stops in the points where the Nc value of the point itself and the NC's of neighbouring points differ less than an adjustable threshold value.

By applying this program to the matrix (18), some different local minima (obtained by varying the starting points) have been found. The parameters corresponding to these local minima are reported below.

	LOCAL MINIMA			ACTUAL DIMENSIONS
R	4.1	6.6	7.2	5.0
Q	11.5°	19.5°	20.0°	14.0°
d	9.7	13.5	14.6	10.0
Nc	4.9	3.7	3.6	4.2

While the best choice for Q, d and R would have been the third column (Nc = 3.6), we traded off a little accuracy in order to comply with practical fabrication constraints. Thus, we chose the design parameters R=5mm, d=11mm, Q=14° corresponding to Nc=4.2

Actually, the basic configuration illustrated in Figure 4 has not been chosen only for reducing the dimensionality of the design problem. In fact, by premultiplying both terms of the equation describing the sensor, $\underline{V} = C\underline{P}$ by the matrix M:

$$M = \begin{bmatrix} 1 & 1 & 1 & 1 & 0 & 0 \\ -1 & 0 & 0 & 0 & 1 & 0 \\ 0 & 1 & 0 & 0 & 0 & -1 \\ -1 & 1 & -1 & 1 & 0 & 0 \\ 1 & 0 & -1 & 0 & 0 & 0 \\ 0 & 1 & 0 & -1 & 0 & 0 \end{bmatrix} \qquad 19)$$

we obtain

$$M\underline{V} = \begin{bmatrix} V_1+V_2+V_3+V_4 \\ V_5-V_1 \\ V_2-V_6 \\ V_2-V_1+V_4-V_3 \\ V_1-V_3 \\ V_2-V_4 \end{bmatrix} = MC\underline{P} = \begin{bmatrix} 4C_1 & 0 & 0 & 0 & 0 & 0 \\ 0 & C_7 & 0 & 0 & 0 & 0 \\ 0 & 0 & C_8 & 0 & 0 & 0 \\ 0 & 0 & 0 & 4C_4 & 0 & 0 \\ 0 & -2C_2 & 0 & 0 & 2C_5 & 0 \\ 0 & 0 & 2C_3 & 0 & 0 & 2C_6 \end{bmatrix} \underline{P} \qquad 20)$$

Thus, an almost uncoupled sensor is obtained with the same hardware, allowing shorter time response by reducing the computational burden associated with the solution of the linear system.

The different algorithms which solve the linear system associated with the sensor can be implemented in subroutines invoked alternatively, according to the prevalence of either accuracy or response swiftness requirements in the current task phase.

Of course, the accuracy of force measurement is strongly dependent, in this case, on how well the real sensor matrix approximates (16). In fact, the actual MC matrix (estimated by means of appropriate calibration procedures) will have small elements instead of the expected zeroes, since machining the sensor body, bonding the transducers, etc. will not allow the exact elimination of the Cij. In order to use the fast force sensing method, these small quantities must be ignored, and the corresponding error will add to calibration inaccuracies; the overall error $\|dMC\|/\|MC\|$, propagating to the solution in accordance to (14), will be normally much larger than the original $\|dC\|/\|C\|$, emphasizing constructive inaccuracies.

EXPERIMENTAL

As a first implementation of the above considerations on the design of the force sensor element of an ITS, a prototype fingertip incorporating the ITS has been realized in our laboratory. The fingertip was designed in view of a future integration with an ETS.

The present prototype consists of a hollow cylinder made out of aluminum alloy, which supports a sphere at one end. As depicted in Figure 2, a flange located at the other end connects the fingertip to the distal phalanx of an articulated finger |Bicchi 1984||Dario et al. 1985|.

Six foil-type strain gauges are bonded to a thin walled portion of the cylinder, according to the disposition shown in Figure 3 and to the dimensional data reported above. A seventh strain gauge is fixed to a part of the cylinder having much thicker wall, so that its output can be used to compensate for possible thermal drift.

The thickness of the thin walled cylinder has been dimensioned to withstand a maximum load of 30 N (it should be noted that the wall thickness does not affect the sensor Condition Number, i.e. its accuracy); if larger bending loads are applied orthogonal to the cylinder axis, the cylinder is prevented from collapsing by a stiff coaxial cylinder.

The force sensor fits into a cylindrical cavity in the sphere. The center of the sphere (that is the active surface of the ITS) lies in the same plane as the centers of the strain gauges in the first row.

The sphere radius is 13 mm; the active surface (where contacts can be detected) is 92% of the sphere surface, corresponding to a solid angle of 11,58 spherical radians.

Each strain gauge is individually wired in a Wheatstone quarter-bridge arrangement; the bridge output is amplified, A/D converted and sent to a DEC PDP 11/73 computer.

Some experimental tests have been carried out in order to assess sensor performances. Although neither very accurate construction or precise instrumentation were used in the present prototype, experimental results were fairly good, probably owing to the "robust" design resulting from the condition number approach.

The accuracy of force measurement in the prototype was about 2% of the measured value; the minimum detectable force was 0.1 N.

The location of the contact point can be calculated with a precision variable with the intensity of the contact force: Figure 5 (a)(b) shows the graphic displays corresponding to a point contact load of 1 N and 10 N, respectively, on the top of the fingertip sphere.

The measured forces were, respectively, 1.0 N and 10.1 N; the position errors were, respectively, 0.2 mm and 0.05 mm. For the general case of a contact force in the range 0.1 N-30 N, the precision is better than 1 mm.

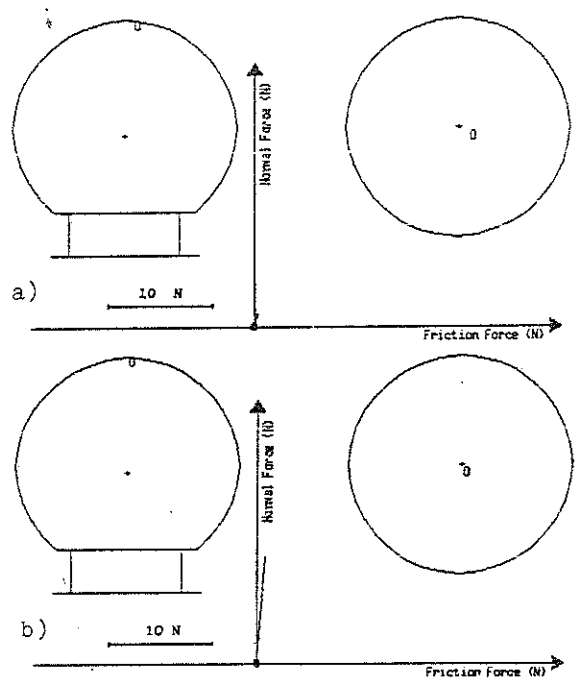

FIG. 5 (a,b). The graphic display of two experimental tests, showing the calculated position of the contact point and the contact force components for two different loads.

Finally, some preliminary experiments have been carried out in order to evaluate the feasibility of slippage control through IT sensing. A plane surface was pressed against the sensor with constant normal force, while an increasing force tended to slide the surface over the sensor. Resultant normal and tangential forces on the fingertip surface were monitored; the ratio, Rnt, between normal and tangential force is plotted vs. time in Figure 6, referring to the case of a rubber surface.

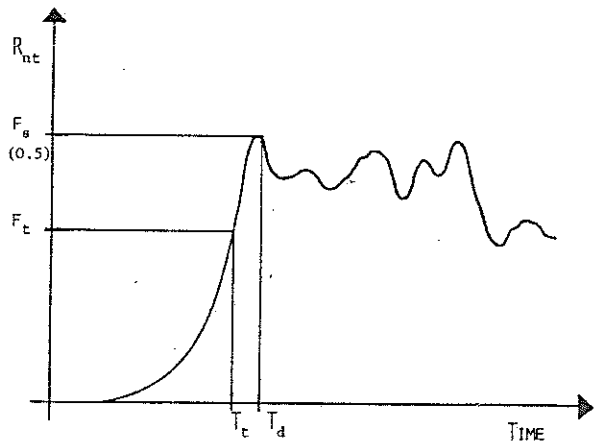

FIG. 6. Monitoring of friction and slippage by the ITS.

As the sliding force increases, the contact opposes an increasing counteracting friction force, until, at time Td, the static friction coefficient (Fs) is overcome and stick-slip occurs.

Two slippage control modes are possible. A first strategy is appropriate when the material and the superficial characteristics of the manipulated objects have been experimentally evaluated in advance. By comparing current Rnt ratios measured during the manipulation tasks, with a threshold value set on the basis of a safe estimate of Fs , adequate actions can be undertaken by the controller. In the general case in which object properties are not known a priori, slippage detection is still possible by detecting the abrupt variations of the Rnt ratio due to the first occurrence of dynamic friction.

CONCLUSIONS

The approach to tactile sensing presented in this paper has, in principle, general validity: an ITS is capable of detecting data on the contact between the end effector and the manipulated object informative and accurate enough to allow the controller not only to manage manipulation tasks, but also to infer information useful for perceptual purposes. As anticipated in the introduction, however, since the peculiar characteristics of the ITS are reliability, robustness and fast operation, while the main (although, at present, mostly potential) advantages of ETS are their capability of measuring locally minute stress or strain, and their sensitivity to physical and chemical parameters other than force, an ideal configuration of an advanced robot hand would include both types of sensors. In such configuration, the primary role of the ITS would be providing data useful for the low level control of manipulation, while the function of the ETS should be detecting exteroceptive data on the manipulated object. According to this schematization, that has some analogies with the organization of the nervous central system in humans, the accurate control of contact conditions is a prerequisite to true tactile exploration |Bicchi et al. 1985||Dario and Buttazzo 1987|. While the ITS measures accurately the overall contact conditions, as is actually necessary in order to carry out any manipulative task, an ETS located at the fingertip surface can sense a number of significant parameters relative to the local features of the explored object. If we accept the anthropomorphic analogy, we could tolerate that the accuracy of some of the measurements obtained by the ETS is relatively low: in fact, provided that a substantial level of intelligence is incorporated in the top levels of the hierarchical control, even semiqualitative, redundant information could be organized in order to obtain a coherent model of the explored object.

In order to verify the practical value of this approach, we have designed a testbed for the analysis of the fundamentals of haptic perception which is intended to implement most of the concepts outlined above. The main component of the experimental testbed is an articulated robot finger incorporating many different sensors, each having a primary function distinct from that of the other sensors. However, some of the data provided by the different sensors,

just like in biological systems, may overlap. Devising appropriate methods and techniques for dealing with sensor redundancy in the proposed robot system are the ultimate goal of this research.

Figure 7 illustrates a scheme of the version of the fingertip being currently developed |Dario et al. 1987|. The fingertip incorporates the ITS presented in this paper, and a new ETS comprising, at present, an optical tactile sensor capable of measuring locally the normal and tangential components of contact forces |Femi et al. 1987|, as well as an array of undulated, piezoelectric polymer film transducers for ultrasonic imaging. A further interesting feature of the new finger is the shape memory alloy-based actuator located within the phalanxes, that, allowing to eliminate most of the tendon routings, is specifically intended for generating the smooth motions required for fine manipulation.

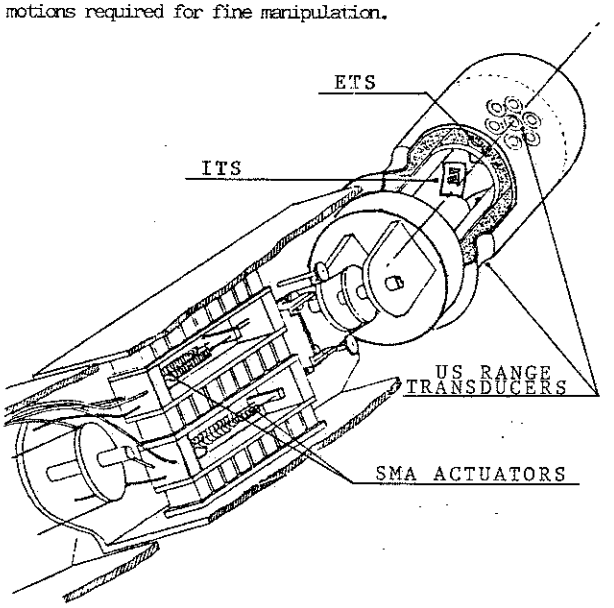

Fig. 7. Schematic view of a sensorized fingertip incorporating both the ITS described in this paper and a new ETS.

ACKNOWLEDGMENTS

The authors wish to thank G. Vassura for helpful discussions on the design of the ITS, and F. Vivaldi for the technical assistance in sensor fabrication.

The work described in this paper was supported in part by the Italian Government (MPI 40%), and by NATO Scientific Affairs Division (C.R.G. 224/85).

REFERENCES

Bejczy, A.K., "Smart hand-Manipulator control through sensory feedback," JPL D-107 Report, January 15, 1983.

Bicchi, A., Thesis for the Doctor's Degree in Mechanical Engineering on "Design of a pluriarticulated finger for tactile exploration", University of Pisa, Italy, 1984.

Bicchi, A., Dario, P., Pinotti, P.C., "On the Control of a Sensorized Artificial Finger for Tactile Exploration of Objects," Robot Control (SYROCO '85)", Edited by L. Basanez, G. Ferraté, G.N. Saridis. IFAC Publication-Pergamon books Ltd, pp. 251-256.

Brock, D., Chiu, S., "Environment perception of an articulated robot hand using contact sensors," Proc. ASME Winter Annual Meeting, Miam, Nov. 1985.

Dario, P., De Rossi, D., Domenici, C., Francesconi, R., "Ferroelectric polymer tactile sensors with anthropomorphic features," Proc. 1st IEEE int. Conf. on Robotics, Atlanta, GA, pp. 332-340, March 1984.

Dario, P., Bicchi, A., Vivaldi, F., Pinotti, P.C., "Tendon actuated exploratory finger with polymeric, skin-like tactile sensor. Proc. 2nd IEEE Int. Conf. on Robotics and Automation, St. Louis, pp. 701-706, March 1985.

Dario, P., "Contact sensing for robot active touch, "Proc. SDF Benchmark Symp. on Robotics Research, Santa Cruz, CA, MIT Press, Aug. 1987.

Dario, P., Bicchi, A., Femi, D., Fiorillo, A.: "Multiple sensing fingertip for robot active touch," Proc. of 3rd Int. Conf. on Advanced Robots, Versailles, Oct. 1987.

Dario, P. and Buttazzo, G.: "An anthropomorphic robot finger for investigating artificial tactile perception". Int. J. Robotics Res., 1987.

Femi, D., Dario, P., Lombardi, P., Francesconi, R.: "An optical fiber-based multicomponent tactile sensor", Proc. 10th IASTED Int. Symp. on Robotics and Automation, Lugano, June 1987.

Harmon, L.D., "Automated tactile sensing," Int. J. Robotics Res., Vol. 1, No. 2, pp. 3-32, 1982.

Hirzinger, G., "The space and telerobotic concepts of DFVLR rotex," Proc. IEEE Int. Conf. on Robotics and Automation, Raleigh, NC, pp. 443-449, March 1987.

Salisbury, J.K., "Interpretation of contact geometries from force measurements," Proc. 1st Int. Symp. on Robotics Research, Bretton Woods, NH, MIT Press, Sept. 1984.

Siegel, D.M., Garabieta, I., Hollerbach, J.M., "An integrated tactile and thermal sensor", Proc. IEEE Int. Conf. on Robotics and Automation, San Francisco, CA, pp. 1286, 1291, April 1986.

Von Brussel, H., Belien, H., Thielemans, H., "Force sensing for advanced robot control," Proc. 5th Conf. on Robot Vision and Sensory Control, Amsterdam, pp. 59-68, Oct. 1985.

Wilkinson, J.H., "The algebraic eigenvalue problem," Clarendon Press, Oxford 1965.